JOURNAL OF BACTERIOLOGY, Oct. 1990, p. 5938–5948
0021-9193/90/105938-11$02.00/0

Vol 172, No. 10

Organization of Dimethyl Sulfoxide Reductase in the Plasma Membrane of *Escherichia coli*

D. SAMBASIVARAO, DOUGLAS G. SCRABA, CATHARINE TRIEBER, AND JOEL H. WEINER*

Department of Biochemistry, University of Alberta, Edmonton, Alberta, Canada T6G 2H7

Received 15 May 1990/Accepted 2 August 1990

Dimethyl sulfoxide reductase is a trimeric, membrane-bound, iron-sulfur molybdoenzyme induced in *Escherichia coli* under anaerobic growth conditions. The enzyme catalyzes the reduction of dimethyl sulfoxide, trimethylamine *N*-oxide, and a variety of *S*- and *N*-oxide compounds. The topology of dimethyl sulfoxide reductase subunits was probed by a combination of techniques. Immunoblot analysis of the periplasmic proteins from the osmotic shock and chloroform wash fluids indicated that the subunits were not free in the periplasm. The reductase was susceptible to proteases in everted membrane vesicles, but the enzyme in outer membrane-permeabilized cells became protease sensitive only after detergent solubilization of the *E. coli* plasma membrane. Lactoperoxidase catalyzed the iodination of each of the three subunits in an everted membrane vesicle preparation. Antibodies to dimethyl sulfoxide reductase and fumarate reductase specifically agglutinated the everted membrane vesicles. No Tn*phoA* fusions could be found in the *dmsA* or *-B* genes, indicating that these subunits were not translocated to the periplasm. Immunogold electron microscopy of everted membrane vesicles and thin sections by using antibodies to the DmsABC, DmsA, or DmsB subunits resulted in specific labeling of the cytoplasmic surface of the inner membrane. These results show that the DmsA (catalytic subunit) and DmsB (electron transfer subunit) are membrane-extrinsic subunits facing the cytoplasmic side of the plasma membrane.

Dimethyl sulfoxide (DMSO) reductase of *Escherichia coli* (5) is a terminal enzyme expressed constitutively under anaerobic conditions and is capable of reducing DMSO and trimethylamine-*N*-oxide (TMAO). We have reported that the *E. coli* DMSO reductase is a membrane-bound iron-sulfur molybdoenzyme genetically distinct from the single or dual subunit forms of TMAO reductase (40). The structural genes encoding the enzyme have been cloned, and their DNA sequences have been determined (4, 7). The enzyme has been purified to homogeneity and shown to be composed of three nonidentical subunits: a catalytic subunit (DmsA; 82,600 daltons), an iron-sulfur subunit (DmsB; 23,600 daltons), and a membrane anchor subunit (DmsC; 22,700 daltons).

The presence of one constitutive and three inducible forms of TMAO reductase have been demonstrated (32, 36, 42); however, the significance and precise localization of these multiple forms of TMAO reductase in the energy transduction mechanisms of the cell are not clear. The enzymes responsible for TMAO and DMSO reduction in certain marine organisms and nonphotosynthetic bacteria have been characterized in some detail (2). A single enzyme in *Rhodobacter* sp. has been found to be responsible for the reduction of both DMSO and TMAO (23). The reductases in these organisms were found to be localized in the periplasmic compartment. The pathway of electron transfer to the periplasmically localized reductases and a concommitant vectorial proton translocation mechanism are at present speculative (28).

It was noted that the *dmsA* gene codes for a 16-residue peptide at the amino terminus of DmsA which is absent from the purified protein and which resembles bacterial signal sequences (4, 7). This suggests that the DmsA subunit may be translocated to the periplasmic compartment. Observation of periplasmically localized *b* and *c* types of cytochromes in *E. coli* grown anaerobically with TMAO further strengthened the arguments for the association of these DMSO- and TMAO-terminal reductases with the periplasmic compartment (8). These observations led us to explore the topology of DMSO reductase in normal cells and in cells overexpressing the *dms* operon. The topological characterization of DMSO reductase reported here is based on biochemical, immunological, and electron microscopic techniques coupled with comparative studies with *E. coli* fumarate reductase, which is known to have both catalytic subunits on the cytoplasmic face of the plasma membrane (10). The sum of our studies leads us to conclude that the catalytic DmsA and electron transfer DmsB subunits bind to DmsC on the cytoplasmic face of the plasma membrane.

MATERIALS AND METHODS

Chemicals and reagents. Benzyl viologen, methyl viologen, fumarate, dithiothreitol, sucrose, EDTA, TMAO, *N*-α-*p*-tosyl-L-lysine chloromethyl ketone-treated α-chymotrypsin, morpholinepropanesulfonic acid (MOPS), and proteinase K were obtained from Sigma Chemical Co., St. Louis, Mo. DMSO was obtained from Fisher Scientific Ltd., Edmonton, Alberta, Canada. Bovine serum albumin and Pansorbin (glutaraldehyde-fixed *Staphylococcus aureus* cells in a 10% [wt/vol] suspension) were purchased from Calbiochem-Behring, La Jolla, Calif. Carrier-free ^{125}I, in a solution of 0.1 M NaOH, was obtained from the Radiopharmaceutical Centre, Edmonton, Canada. The electrophoretic apparatus and reagents for Western immunoblotting were obtained from Bio-Rad Laboratories, Richmond, Calif. The colloidal gold-labeled goat anti-rabbit immunoglobulin G (IgG) (auroprobe EM, 10-nm gold particle) was purchased from Janssen Life Sciences Products, Piscataway, N.J. Lowicryl K4M was purchased from Polysciences, Inc., Warrington, Pa. All other reagents were of analytical grade.

Bacterial strains and plasmids. *E. coli* HB101 (F^- *hsdR*

* Corresponding author.

hsdM pro leu gal lac thi recA rpsL) was used throughout the studies reported here. pDMS159 and pFRD84 are recombinant pBR322 plasmids carrying the *E. coli* chromosomal DNA fragment coding for the entire DMSO reductase and fumarate reductase operons, respectively (7, 10).

Growth conditions and preparation of membrane vesicles. *E. coli* HB101, HB101(pDMS159), and HB101(pFRD84) cells were grown anaerobically at 37°C on a glycerol-fumarate minimal medium, supplemented with appropriate antibiotics (5, 39, 40). The cells were harvested at stationary phase, washed, and suspended in 50 mM MOPS buffer (pH 7.5). Membrane vesicles (everted crude membrane vesicles) were prepared by lysing the cells in a French pressure cell, as previously described (5). Purified everted inner membrane vesicles were prepared by the method of Yamato et al. (44), except that the pressure of the French press was set at 16,000 lb/in^2 (110 mPa). The membrane vesicles and inner membrane vesicles were suspended in 50 mM MOPS buffer at a final concentration of 20 to 25 mg of protein ml^{-1} and stored in aliquots at −70°C. All preparations of the membrane vesicles were routinely assayed for protease sensitivity of the cytoplasmic marker, fumarate reductase. We observed that vesicles prepared by French pressure lysis consistently yielded membrane vesicles of inside out orientation (≥75%).

Outer membrane-permeabilized cells were prepared by the method of von Heijne et al. (38), except that lysozyme was omitted.

Enzyme assays. Fumarate and DMSO reductase activities were determined by monitoring the substrate-dependent oxidation of reduced benzyl viologen at 570 nm (5; R. Cammack and J. H. Weiner, Biochemistry, in press). TMAO (70 mM) was routinely used as a substrate for the DMSO reductase assay, since it has been shown to have at least a threefold-higher turnover than DMSO (40). Studies with both substrates indicate that the TMAO reductase activity of DMSO reductase accounts for 90% of the total TMAO reductase activity in the cells (D. Sambasivarao and J. H. Weiner, unpublished data). One unit of reductase activity is defined as the oxidation of 1 μmol of benzyl viologen per minute. Specific activity is expressed as units of activity per milligram of protein.

Protease digestion experiments. Proteolysis experiments were carried out in 50 mM MOPS buffer (pH 7.5 at 30°C) or 200 mM Tris hydrochloride buffer (pH 8.0 at 37°C) unless specified otherwise. The proteolysis in the outer membrane-permeabilized cells was carried out in 50 mM Tris hydrochloride, pH 8.0. Chymotrypsin and proteinase K were made as 1 mg/ml stock solutions in 50 mM MOPS buffer, pH 7.5. Protease-to-reductase ratios were as indicated in the figure legends. Samples (5 to 50 μl) were removed at various intervals for enzyme activity measurements. Subunit analysis was carried out by electrophoretic techniques, as previously described (24, 38, 40).

Polyclonal antibodies. Polyclonal antibodies were raised in rabbits by using either purified DMSO reductase (DmsABC) or electroeluted DmsA and DmsB subunits as antigens. Electroelution of the individual subunits from sodium dodecyl sulfate-polyacrylamide gels was carried out as previously described (18). Polyclonal antibodies to the FrdAB, FrdA, and FrdB subunits of fumarate reductase were raised in rabbits, as previously described (25). The IgG fraction was purified by ammonium sulfate precipitation and DEAE chromatography (9). Immunoblotting (with purified IgG) was carried out according to the procedure of Renart et al. (33), by using horseradish peroxidase. Affinity-purified antibodies for the DmsA and DmsB subunits were prepared from anti-DmsABC antibodies by using the protein immobilized on nitrocellulose paper as an absorbant (37).

Antibody-mediated agglutination of membrane vesicles. Membrane vesicles prepared from strains HB101, HB101 (pDMS159), and HB101(pFRD84) were incubated with anti-DMSO reductase (in the presence of TMAO) and anti-fumarate reductase antibodies (in the absence of the substrates) at the specified protein-to-antibody ratios. The incubation buffer, temperature, and the duration of incubation were as previously described (15, 17).

Iodination of purified DMSO reductase and membrane vesicles. One unit of lactoperoxidase plus 66 μCi of neutralized carrier-free ^{125}I was added to the membrane vesicles (1.0 mg of protein) in a reaction volume of 0.1 ml. The iodination reaction was initiated by the addition of peroxide as previously described (29) and terminated by the addition of 50 mM (final concentration) of β-mercaptoethanol after 2 and 60 min for the purified reductase and the membranes, respectively. The free label was removed by applying the samples onto a Sephadex G-25 column (2.5 by 1 cm) which was preequilibrated with 1.0 mg of bovine serum albumin per ml in 0.2 M potassium phosphate buffer, pH 7.0. The ^{125}I-labeled vesicles were treated with Triton X-100 (2.2%, vol/vol, final concentration) to extract the reductase. A sample of the supernatant fraction of this extract (equivalent to 5 μg of purified reductase) was immunoprecipitated, and the subunits were separated by sodium dodecyl sulfate-polyacrylamide gel electrophoresis. Immunoprecipitations were carried out with the anti-DmsABC antibody and subsequently adsorbed to *S. aureus* cells. The reductase subunits were recovered from the immunoprecipitates as previously described (41).

Generation of Tn*phoA* fusions. The alkaline phosphatase gene fusions were generated as described by Manoil and Beckwith (26) by infecting λTn*phoA* into *E. coli* CC118 (pDMS159).

Immunogold staining and negative stain electron microscopy. The purified inner membrane vesicles prepared from HB101 or HB101(pDMS159) were adsorbed to hydrophilic carbon films on copper mesh grids and reacted with the specified primary and secondary gold-conjugated antibodies (12).

Immunoelectron microscopy of thin sections. Samples of cells from HB101 or HB101(pDMS159) grown for 48 h on glycerol-fumarate minimal medium were harvested by centrifugation. All incubations and washes were done in phosphate-buffered saline and/or phosphate-buffered saline containing solutions at room temperature. The washed cell pellets were fixed in a mixture of 2% (wt/vol) formaldehyde (freshly prepared from paraformaldehyde) and 0.1% (vol/vol) glutaraldehyde for 60 min. Fixed cells were washed, incubated, and embedded in lowicryl K4M, as previously described (35). Thin sections mounted on carbon films on nickel grids were incubated with phosphate-buffered saline–bovine serum albumin and primary and secondary (colloidal gold-conjugates) antibodies and stained with 0.05% (wt/vol) uranyl acetate and Reynold lead citrate (35).

Release of periplasmic proteins from *E. coli*. Periplasmic proteins from HB101 grown on glycerol-fumarate minimal medium for 48 h were released by cold osmotic shock (30) or by chloroform wash (1). Controls were done by incubating the cells in 30 mM Tris hydrochloride (pH 7.0) for a length of time corresponding to the osmotic shock and chloroform wash experiments. The Tris wash, shock fluid, or aqueous

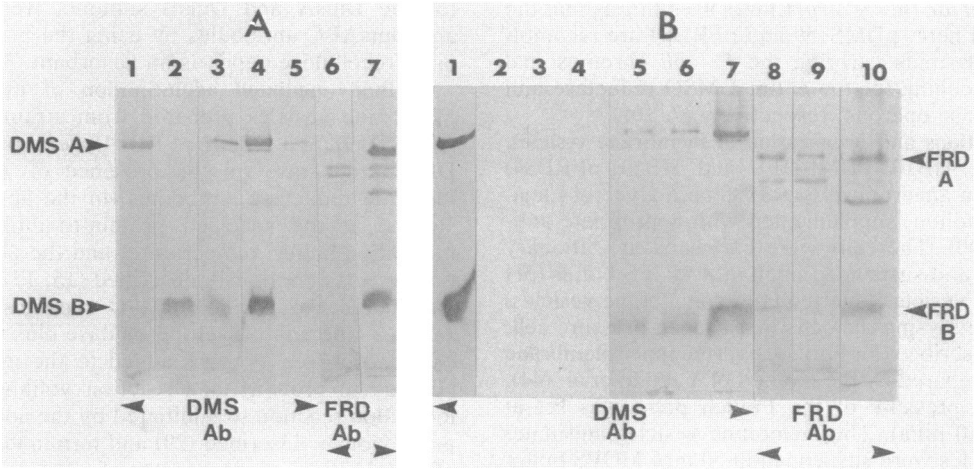

FIG. 1. Immunoblot identification of DmsAB and FrdAB. (A) Proteins resolved on a 12% polyacrylamide gel were immunoblotted as described in Materials and Methods. Lanes 1 and 2, Purified DMSO reductase (1.2 μg) probed with the anti-DmsA and anti-DmsB antibodies, respectively. Proteins from whole cells of HB101 (lane 3), HB101(pDMS159) (lane 4), and HB101(pFRD84) (lane 5) were reacted with a mixture of 1:500 diluted (1 mg of IgG stock per ml) anti-DmsA and anti-DmsB antibodies. Proteins from whole cells of HB101(pDMS159) (lane 6) and HB101(pFRD84) membranes (lane 7) were probed with a mixture of similarly diluted anti-FrdA and anti-FrdB antibodies. The DmsA and the smeary DmsB subunits are indicated by arrows. The reasons for the smeary nature of DmsB are not known. The 45 to 60-kilodalton bands seen with Frd antibodies are presumably the degradation products of the FrdA subunit, as they reacted only with the anti-FrdA antibodies. Protein was loaded at 20 μg per lane (lanes 3 to 7) and represents less than 0.1% of total cellular protein. (B) Analysis of bacterial periplasmic fractions for fumarate and DMSO reductase. Proteins released by various treatments were resolved on 12% sodium dodecyl sulfate-polyacrylamide gels and transferred to nitrocellulose paper, as described in Materials and Methods. Lane 1, Purified DMSO reductase; lanes 2 to 4, HB101; lanes 5 to 7, HB101(pDMS159); lanes 8 to 10, HB101(pFRD84). Lanes 2, 5, and 8, Supernatant fractions from buffer wash; lanes 3, 6, and 9, osmotic shock fluid; lanes 4, 7, and 10, chloroform wash fluid. Protein from HB101 (15 μg) and from HB101(pDMS159) or HB101(pFRD84) (20 μg) were loaded on each lane and blotted with the antibodies as indicated. The amount of protein loaded per lane makes up approximately 4.5 and 3% of the total recovered periplasmic protein fractions from the osmotic shock and chloroform wash procedures, respectively.

phase from the chloroform wash were concentrated by Centricon microconcentrators.

Protein determination. Protein was estimated by a modification by Markwell et al. (27) of the Lowry procedure, with bovine serum albumin as a protein standard.

RESULTS

Immunoblot identification of the DmsAB and FrdAB subunits. Polyclonal antibodies raised individually against the DmsA and DmsB subunits and the FrdAB subunits of fumarate reductase were used to identify the Dms and Frd polypeptides. Unfortunately, the hydrophobic subunit, DmsC, did not transfer to the nitrocellulose membrane under a wide variety of experimental conditions and could not be examined in this study. An immunoblot of purified DMSO reductase (Fig. 1A, lanes 1 and 2) as well as fumarate and DMSO reductases from cells showed that the DmsA and B subunits could be observed in both normal (HB101; Fig. 1A, lane 3) and overexpressing cells [HB101(pDMS159); Fig. 1A, lane 4]. As expected, the bands were much more prominent in the overexpressing cells. DmsAB could also be observed in cells overexpressing fumarate reductase [HB101(pFRD84); Fig. 1A, lane 5] even though fumarate reductase is greatly overexpressed in these cells and can account for up to 90% of the membrane protein (10). Fumarate reductase was observed in cells overexpressing this enzyme [HB101(pFRD84); Fig. 1A, lane 7] but not in HB101(pDMS159) at the protein concentrations tested. There was no cross-reactivity between the anti-fumarate reductase and anti-DMSO reductase antibodies or the heterologous enzymes.

Release of proteins from the periplasmic space. Osmotic shock and chloroform wash treatments of *E. coli* cells are known to selectively release binding proteins and enzymes from the periplasmic space (1, 30). We used these procedures to test whether any of the DmsAB subunits were free in the periplasm or easily dislodged from the periplasmic side of the plasma membrane (Fig. 1B). The FrdAB subunits which are known to be on the cytoplasmic side of the plasma membrane were also examined. The major findings from these experiments are as follows. (i) Of the total cellular protein, 10 to 15% was released upon osmotic shock and chloroform wash comprising the periplasmic fraction (30). (ii) There was no detectable activity of either reductase in the osmotic shock fluids. (iii) Neither DmsAB (Fig. 1B, lanes 2 to 4) nor FrdAB (not shown) was seen in immunoblots for any of the osmotic shock fluids from HB101. (iv) The control or osmotic shock fluids from the amplified strains showed identical intensities of the subunits for both the reductases (Fig. 1B, lanes 5 versus 6 and 8 versus 9). This is probably due to a small amount of cell lysis during the incubation period. (v) The chloroform wash fluids contained larger amounts of both reductase subunits (Fig. 1B, lanes 7 and 10). This was likely due to increased cell lysis during the chloroform treatment. Release of small amounts of cytoplasmic proteins during the chloroform shock treatment has been reported by Ames et al. (1). The immunoblot profiles of fumarate reductase (Fig. 1B), a cytoplasmically localized enzyme, further confirm these observations. Together, these results suggest that the DmsA and B proteins were not soluble in the periplasm or weakly bound to the periplasmic side of the membrane.

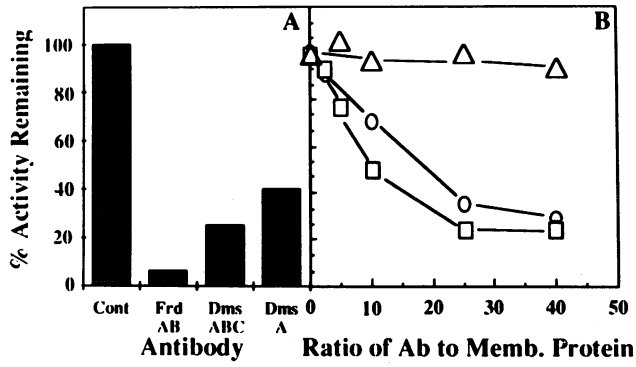

FIG. 2. Agglutination of the membrane vesicles with the anti-fumarate reductase and anti-DMSO reductase antibodies. (A) Agglutination of membrane vesicles derived from *E. coli* HB101. Membrane vesicles (250 μg of protein) were incubated separately with the purified IgG from preimmune sera (Cont), anti-fumarate reductase (Frd AB), anti-DMSO reductase (Dms ABC), and anti-DmsA (DmsA) subunits at protein-to-IgG ratios (wt/wt) as follows: 1:40, control; 1:20, FrdAB and DmsABC; and 1:30, DmsA. After incubation (16 h at 4°C), the antigen-antibody mixture was centrifuged (13,000 × *g*, 10 min) to remove the agglutinated material. The supernatant fractions (nonagglutinated vesicles) were assayed for fumarate and DMSO reductase activities, as described in Materials and Methods. Data is expressed as percent activity remaining in the supernatant fraction, with 100% activity corresponding to 6.84 and 3.5 U/mg of DMSO reductase and fumarate reductase, respectively. (B) Titration of fumarate and DMSO reductase activity in membrane vesicles from HB101(pDMS159) as a function of antibody (Ab) concentration. Membrane (Memb.) vesicles (250 μg of protein) were incubated separately with anti-FrdAB antibody (□), anti-DmsABC antibody (○), or IgG from preimmune serum (△) at the indicated protein-to-antibody ratios. Activities for fumarate and DMSO reductases were identical in the control as a function of IgG concentration and are therefore shown as a single curve. Individual enzyme activities in the nonagglutinated vesicles were determined as described above. One hundred percent activity corresponds to 4 U/mg for fumarate reductase and 190 U/mg for DMSO reductase.

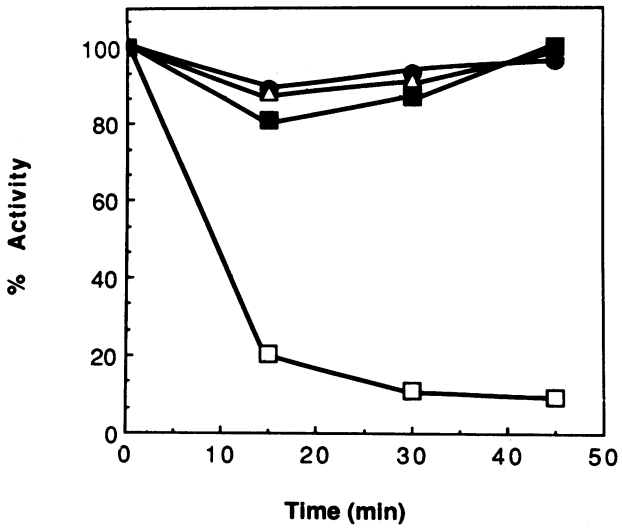

FIG. 3. Effects of proteinase K on the activity of DMSO reductase in outer membrane-permeabilized cells prepared from HB101 (pDMS159). The permeabilized cells were incubated with proteinase K (at a protease-to-reductase ratio [wt/wt] of 1:4) at 0°C for 30 min to facilitate protease entry into the periplasmic compartment. During this time, no loss of activity was noted in the cells, and this value was taken as the zero time measurement for the subsequent incubation at 30°C. Reductase activities in the outer membrane-permeabilized cells were monitored by using reduced benzyl viologen and TMAO as the electron donor and acceptor, respectively. Proteinase K only, ●; untreated, permeabilized cells (control), △; Triton X-100 only, ■; Triton X-100 and proteinase K, □. Triton X-100 was used at a final concentration of 2.0% (vol/vol). Total reaction volume of the digestion mixture was 1.75 ml. One hundred percent activity corresponds to 5.1 U/mg.

Orientation of DMSO reductase in membrane vesicles. Membrane vesicles prepared by French press lysis of *E. coli* cells are predominantly everted with respect to whole cells (34). The orientation of cytoplasmically localized enzymes in such vesicle preparations can be studied by techniques based on the accessibility of the enzyme to proteases, inhibitors, impermeable substrates, or antibodies. We used antibodies to elucidate the topology of DMSO reductase on the basis of the following premise. Antibodies to cytoplasmically localized enzymes, when added to membrane vesicles, would lead to the agglutination of the population of vesicles which are inside out in orientation. The activities remaining in the nonagglutinated vesicles after centrifugation would reflect the population of vesicles that are of the same orientation as intact cells. This method has been used by others to demonstrate both the heterogeneity of vesicle preparations and the orientation of specific enzymes in vesicles prepared by various methods (15, 17).

The activities of fumarate reductase and DMSO reductase in nonagglutinated membrane vesicles following incubation with specific antibodies (Fig. 2) can be summarized as follows. (i) There was no agglutination of vesicles prepared from HB101 (Fig. 2A) or HB101(pDMS159) (Fig. 2B) treated with IgG from preimmune sera. (ii) Addition of anti-FrdAB led to the agglutination of 90 and 75% of the vesicles derived from HB101 and HB101(pDMS159), respectively. (iii) Anti-DMSO reductase antibody precipitated 75% of the membrane-bound reductase activity in both strains, whereas anti-DmsA caused 60% of the vesicles to agglutinate in the normal strain (Fig. 2A) at the antibody concentrations tested (1:20 and 1:30, respectively). A systematic antibody titration was not attempted in the normal strain, because of the low level of DMSO reductase activity; however, Fig. 1A indicates that the orientation of the DMSO reductase was the same as that of fumarate reductase. (iv) Anti-DMSO reductase and anti-fumarate reductase antibodies had no direct inhibitory action on the activities of the membrane-bound reductases at the concentrations used in this study. The activity of the purified DMSO reductase was also found resistant to the action of the anti-DMSO antibodies (data not shown), indicating that the observed decrease in the reductase activities are due to agglutination of the vesicles. (v) The activities of fumarate and DMSO reductases were coprecipitated when incubated with either of the antibodies (data not shown). Thus, these experiments indicate that at least 75% of the vesicles were inside out in orientation with respect to intact cells and that DMSO reductase was predominantly on the cytoplasmic aspect of the plasma membrane in both normal and overexpressing strains.

Protease sensitivity of DMSO reductase. Figure 3 illustrates the action of proteinase K on outer membrane-permeabilized cells derived from the overexpressing strain. Exposure of the periplasmic aspect of the *E. coli* inner membrane to proteinase K did not result in loss of reductase activity. However, up to 90% of the reductase activity was lost on the addition of Triton X-100 to these cells, indicating that the catalytic activity of DMSO reductase is located on the

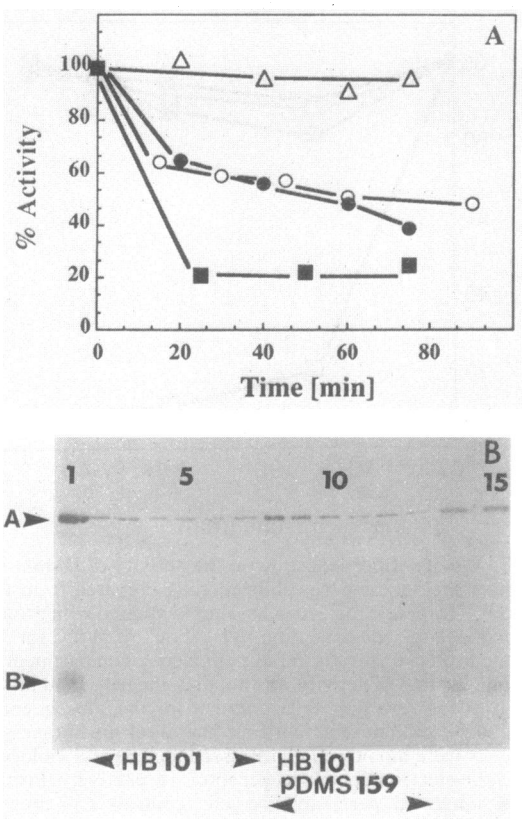

FIG. 4. (A) Effects of proteases on the activities of fumarate and DMSO reductases in membrane vesicles derived from HB101. DMSO reductase digestion was carried out in 200 mM Tris hydrochloride, pH 8.0, at 37°C with a protease-to-reductase ratio of 1:2 (wt/wt). TMAO was used as the substrate. Proteolysis of fumarate reductase with chymotrypsin (■) was carried out at a protease-to-reductase ratio of 1:10 in 50 mM MOPS buffer, pH 7.5. Proteolysis was also carried out for the control without protease for DMSO reductase and fumarate reductase (△) and for DMSO reductase with chymotrypsin (○) or with proteinase K (●). (B) Immunoblot analysis of the chymotrypsin-digested membrane-bound DMSO reductase samples described above. Protein was loaded at amounts of 17.5 μg of HB101 and 2.5 μg of HB101(pDMS159), and immunoblotting was carried out as described in the legend to Fig. 1. Lane 1, Purified DMSO reductase (2.1 μg; the positions of the A and B subunits are indicated); lanes 2 through 7, samples from digestion of HB101 at 1, 15, 30, 45, 60, and 90 min, respectively; lanes 8 through 13, HB101(pDMS159) at identical time intervals; lanes 14 and 15, untreated membrane vesicles from HB101 and HB101(pDMS159), respectively.

cytoplasmic aspect of the inner membrane. The proteolytic inactivation of the reductase could be attributed to the digestion of one or more of the subunits. To address this question, the digestion of the individual subunits was monitored by immunoblotting with everted membrane vesicles prepared from both normal and overexpressing cells treated with proteinase K or chymotrypsin. Enzyme activities for both fumarate reductase and DMSO reductase were monitored at various times during the proteolysis experiments (Fig. 4A). Up to 80% of the fumarate reductase activity in both preparations was eliminated by proteolysis in 20 to 25 min. In comparison, only 50 to 60% of the DMSO reductase activity was lost from membrane vesicles derived from HB101 by treatment with chymotrypsin or proteinase K. Similar protease digestion profiles were obtained for the DMSO reductase and fumarate reductase activities in the vesicles derived from HB101(pDMS159) (data not shown).

Samples obtained at various times during the proteolysis experiments were electrophoresed and immunoblotted in order to determine the susceptibility of the various subunits to chymotrypsin. Figure 4B shows the DmsAB subunits on the immunoblot for both the normal and amplified strains at various times of incubation with chymotrypsin. The amounts of both extrinsic subunits of DMSO reductase decreased gradually as a function of time and correlated with the loss of enzyme activity. DmsC was not amenable to analysis, as it did not transfer to the nitrocellulose supports used in the immunoblots. These results indicate that the extrinsic subunits of DMSO reductase are equally accessible to proteolysis in both the normal and amplified strains.

Localization with differentially permeable electron acceptors. Localization of the active sites of a number of enzymes, including nitrate reductase and fumarate reductase of *E. coli* and formate dehydrogenase of *Vibrio succinogenes* (20, 22), have been determined by using membrane-impermeable dyes and inhibitors. The reduced redox dyes benzyl viologen and methyl viologen were shown to be permeable and impermeable artificial electron donors, respectively, with reference to the *E. coli* membrane (20). We found a 12-fold enhancement of the DMSO reductase activity of French pressure-lysed cells compared with intact cells of HB101 (pDMS159) when DMSO and methyl viologen were used as an electron acceptor and donor, respectively (1.08 versus 0.09 U/mg). This compares to a 15-fold enhancement of fumarate reductase in the same preparations (0.6 versus 0.04 U/mg). Very little difference was observed with benzyl viologen as an electron donor, in keeping with the permeability of this compound.

Lactoperoxidase-catalyzed radioiodination of membrane-bound and purified DMSO reductase. The orientation of DMSO reductase within the cytoplasmic membrane was investigated by using lactoperoxidase-catalyzed ^{125}I iodination. Membrane-impermeable lactoperoxidase has been shown to form a complex with membrane-extrinsic proteins and to iodinate only the exposed tyrosine and histidine residues (29). The purified and membrane-bound DMSO reductases were iodinated to determine the accessibility of tyrosine and histidine residues in the reductase per se and also to study the topological organization of the individual subunits in the membrane. Purified DMSO reductase is routinely prepared and stored in a buffer containing 0.1% Triton X-100 (40), but the detergent interfered with the iodination reaction. To overcome this problem, we used a partially purified fraction prepared by chromatofocusing followed by gel filtration in the absence of detergent (40). Figure 5 (lane 1) shows the iodination of the partially purified reductase. DmsA is poorly iodinated, compared with DmsB or -C. The amino acid composition of DMSO reductase deduced from its DNA coding sequence indicates that DmsA, -B, and -C contain 35, 11, and 6 tyrosines and 17, 7, and 4 histidines, respectively (4). Despite the high tyrosine and histidine content, the poor labeling of DmsA indicates limited accessibility of these residues in the isolated reductase. Iodination of everted membrane vesicles resulted in the labeling of a number of membrane-bound proteins. Detergent extraction followed by immunoprecipitation with anti-DmsABC antibodies demonstrated the labeling of DmsA, -B, and -C polypeptides (Fig. 5, lane 2). These results suggest that the DMSO reductase is situated on the cytoplasmic side of the *E. coli* inner membrane and exposed to the environment when everted vesicles are prepared.

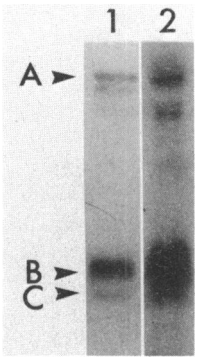

FIG. 5. Iodination of the DMSO reductase. Purified and membrane-bound reductases were iodinated by lactoperoxidase, immunoprecipitated, and autoradiographed as described in Materials and Methods. Lane 1, Iodinated purified reductase (1.5 μg) loaded directly on the gel without immunoprecipitation; lane 2, iodinated everted vesicles treated with Triton X-100 and immunoprecipitated (5 μg equivalent of purified reductase). DmsA, -B and -C subunits are identified by arrows.

Tn*phoA* insertions in the *dms* operon. Transposon Tn*phoA* carries the free alkaline phosphatase gene minus the signal sequence and kanamycin resistance and has been used to construct gene fusions between the *dmsA*, *-B*, or *-C* genes and alkaline phosphatase. Since alkaline phosphatase is only active when assembled in the periplasm, this property can be used to identify proteins which are translocated out of the cytoplasm (26). If DmsA and/or DmsB were located in the periplasm, we would expect to find alkaline phosphatase Dms fusion proteins in this compartment. DNA fusions were constructed as described by Manoil and Beckwith (26). We examined more than 200 independent blue colonies from XP plates by restriction endonuclease digestion. No fusions in *dmsA* or *-B* were identified, although 7% of the clones carried fusions in *dmsC*, as predicted from the transmembranal organization of this subunit. The remainder of the fusions mapped outside the *dms* operon (4). The detailed topology of DmsC will be published elsewhere (D. Sambasivarao, C. Trieber, C. Sedgwick, G. M. Shaw, and J. H. Weiner, unpublished data).

Negative-stain electron microscopy and immunogold labeling. Everted inner membrane vesicles from the DMSO reductase overproducing strain were incubated with anti-DMSO reductase antibodies and then with colloidal gold (10 nm) coated with goat anti-rabbit IgG. Negative-stain electron micrographs of the vesicles labeled with various antibodies are shown in Fig. 6. Panel A shows the vesicles incubated with only the gold-conjugated second antibody. Very few gold particles are found associated with the vesicles or in the background; panel B shows the vesicles treated first with anti-DmsABC antibodies. The micrograph shows some gold label in the vicinity of the vesicles, but most of these gold particles are associated with free proteins adhering to the carbon film. This background labeling could be overcome by passing the vesicles through a Sepharose CL4B column, which removed free protein. The addition of the substrate, 70 mM TMAO (or 20 mM DMSO), to all antibody and washing buffers during the preparation of the samples was found to stabilize the antibody-enzyme complexes. When the vesicles were treated with the affinity-purified antibodies (in the presence of TMAO) to DmsA (Fig. 6, panel C) or DmsB (Fig. 6, panel D), more than 90% of the binding of the antibodies was specifically associated with the exterior surfaces of the membrane vesicles. These studies indicate that both the extrinsic subunits of the DMSO reductase are located on the cytoplasmic side of the *E. coli* plasma membrane and are available for labeling with the individual subunit-specific antibodies in these everted membrane preparations.

Immunogold labeling of DMSO reductase in thin sections. Lowicryl embedding and the immunogold labeling of DMSO reductase in thin sections were as described in Materials and Methods. We included the substrate DMSO during all incubations, as it was found to maintain the integrity of the reductase during the labeling studies. No differences were noted in the labeling when DMSO was replaced with TMAO during the incubations (data not shown). Sections were prepared from both normal and overproducing strains. Figure 7A and B show the gold labeling of the sections from normal and amplified strains incubated in the presence of preimmune IgG. Figure 7C and D show the specific labeling in the presence of anti-DmsABC antibodies for HB101 and HB101(pDMS159), respectively. Sections prepared from the normal strain exhibited very little labeling compared with the amplified strain. The distribution of the gold particles in the amplified strain is in the vicinity of the inner membrane.

A similar distribution of the immunogold-labeled reductase was observed for bacterial sections incubated with anti-DmsA and anti-DmsB antibodies (Fig. 8A, B, and C). These studies were carried out only on thin sections from the amplified strain. Both the polyclonal antibodies prepared against DmsA (Fig. 8A) and the affinity-purified antibodies for DmsA prepared from anti-DmsABC (Fig. 8B) labeled the enzyme near the inner membrane zone, as did polyclonal antibodies for DmsB (Fig. 8C). Of the gold label, 60 to 70% was found to be membrane associated in all cases. The number of immunogold particles associated with the thin sections from the amplified strains was determined from random samples of electron micrographs in four independent experiments. The distribution of the reductase was quantitated from these pooled samples. A similar analysis could not be attempted on the samples obtained from a normal strain because of the small amounts of immunogold labeling on these sections. Data in Table 1 summarize the distribution profiles of the reductase obtained with DmsABC, DmsA, and DmsB antibodies.

The distribution of gold particles near the inner membrane was determined by Ghosh et al. (14) by differential labeling of the enzyme I of the phosphoenolpyruvate system and β-galactosidase of *E. coli*. These authors determined that at least 60 nm from the membrane towards cytoplasm would constitute the inner membrane zone. The observed percent distribution of gold particles for DMSO reductase in the inner membrane zone is approximately the same, irrespective of the antibody used. These studies support the conclusion that DMSO reductase is bound to the inner membrane, with the extrinsic subunits facing the cytoplasmic side.

DISCUSSION

We investigated the topology of DMSO reductase in *E. coli*, because of the following conflicting observations. First, comparison of the inferred amino acid sequence of DmsA with the amino-terminal sequence of the purified subunit indicated that a 16 residue peptide was absent in the latter. The cleavage site of this peptide, Ala-His-Ala//Val-Asp, resembles a typical leader peptidase cleavage site (4). Second, a periplasmic *c* type cytochrome which could participate in an electron transfer chain is observed in cells grown

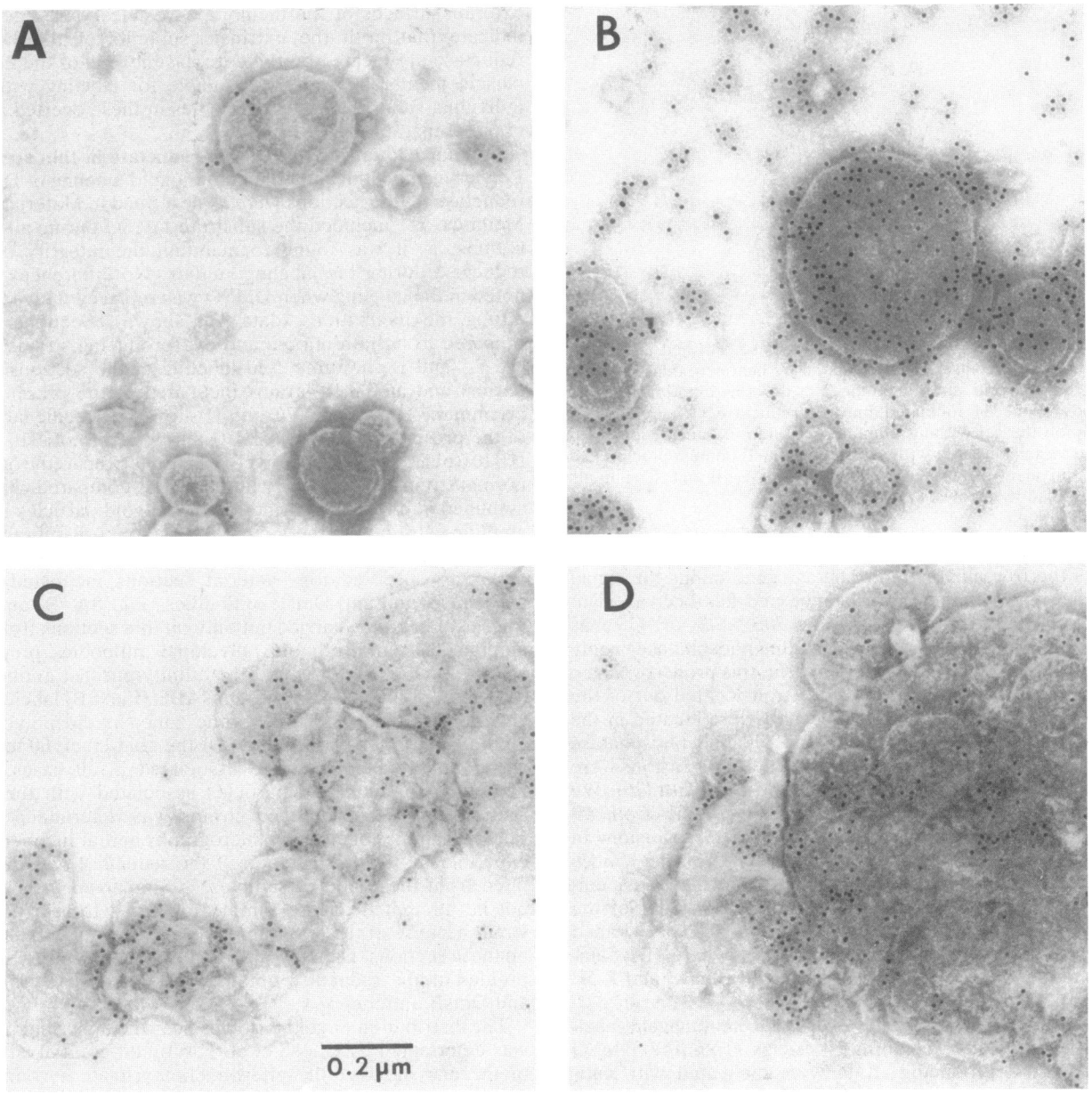

FIG. 6. Negative-stain electron micrographs of *E. coli* HB101(pDMS159) everted inner membrane vesicles. Vesicles were incubated with immunogold reagent (1:25 dilution) in the absence of DMSO reductase antibodies (A) or in the presence of anti-DmsABC (B), anti-DmsA (C), or anti-DmsB (D). Anti-DmsA and anti-DmsB antibodies were purified on an affinity matrix, as described in Materials and Methods. Samples were stained with 1% phosphotungstate and examined in a Philips EM 420 electron microscope operated at 100 kV.

anaerobically on TMAO (8) or DMSO (P. T. Bilous and J. H. Weiner, unpublished data). Third, DMSO reductase has been localized to the periplasm in *Rhodobacter* sp. (23) and other organisms (2). However, a periplasmic localization of DMSO reductase would differ from that found for other terminal anaerobic reductases such as nitrate reductase and fumarate reductase of *E. coli* (16, 19), and proton translocation experiments indicated that DMSO reductase participates in electron transfer in much the same manner as fumarate reductase (6).

In the studies reported here, we used a number of approaches to determine the topology of the DmsA and -B catalytic subunits. Little information could be obtained with respect to DmsC, because of the difficulty in analyzing this polypeptide in immunoblots. Therefore, the topology of this subunit is being investigated by alkaline phosphatase gene fusions (26) (Sambasivarao et al., unpublished data). Interestingly, although we have isolated several fusions in the *dmsC* gene, we have been unable to find any active alkaline phosphatase fusions in *dmsA* or *-B*. This observation supports our contention that these two subunits are not located in the periplasmic space.

We examined the topology of DMSO reductase in normal *E. coli* cells (HB101) and in a strain carrying a recombinant plasmid which overproduces the enzyme to about 30% of total membrane protein [HB101(pDMS159)] in order to see if overexpression modifies the topology. Since fumarate reductase is known to have its catalytic FrdAB subunits on the

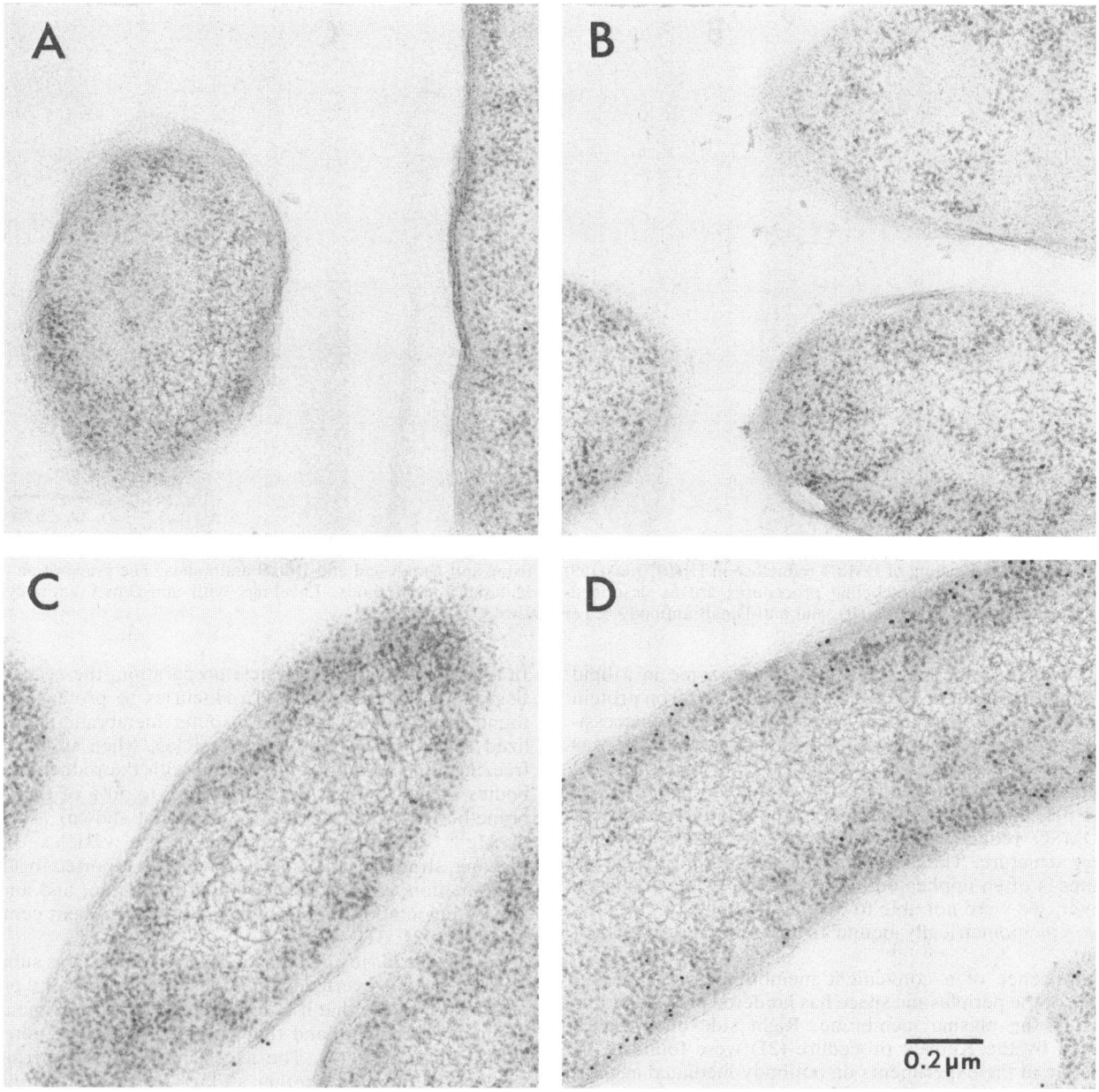

FIG. 7. A comparison of immunolabeling of DMSO reductase in HB101 and HB101(pDMS159). Preparation of cells, immunolabeling of the thin sections of the Lowicryl-embedded cells were as described in Materials and Methods. Sections shown are from HB101 (A) and HB101(pDMS159) (B) treated with IgG from preimmune serum and HB101 (C) and HB101(pDMS159) (D) treated with anti-DmsABC antibody.

cytoplasmic surface, this enzyme was used throughout these studies to account for differences in vesicle sidedness of individual preparations. Taken together, the experimental results indicate that the catalytic subunits of DMSO reductase are also located on the cytoplasmic face of the plasma membrane.

The enzyme was not released from the periplasm by the cold osmotic shock method or by chloroform washing. Although these techniques would not be expected to release DmsA or -B, if they were tightly bound to the periplasmic face of the plasma membrane, we might expect some of the enzyme to be free.

DMSO reductase was not susceptible to protease digestion in outer membrane-permeabilized cells. Only after detergent solubilization of the permeabilized cell plasma membrane did the enzyme become protease sensitive. Membrane vesicles prepared by the French press method have been shown to be predominantly inside out, compared with intact cells (35); in these vesicles, DMSO reductase was protease sensitive, with both DmsA and -B being digested. Qualitatively, it appeared that DmsB was more susceptible than DmsA, but the diffuse migration of DmsB on sodium dodecyl sulfate-polyacrylamide gel electrophoresis made quantitation difficult. Only 50 to 60% of the reductase activity could be destroyed by protease in the vesicle preparation, compared with 90% in detergent-solubilized cells. This difference

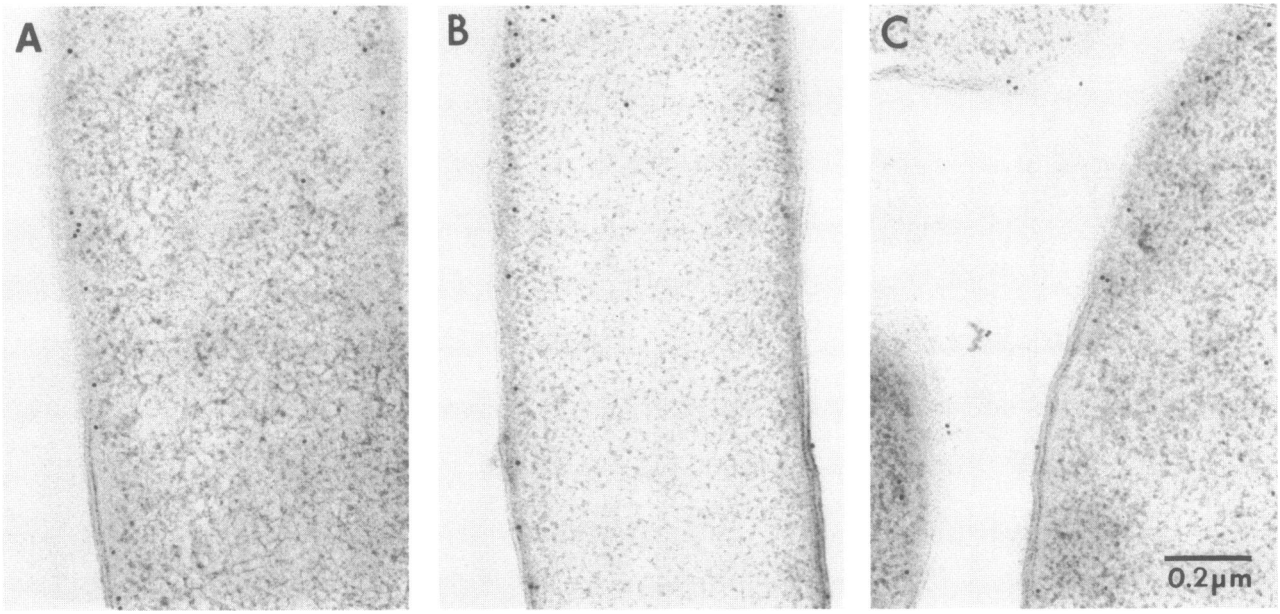

FIG. 8. Immunolabeling of DMSO reductase in HB101(pDM159) by using anti-DmsA and anti-DmsB antibodies. The preparation of the sections, IgG, and immunolabeling procedures are as described in Material and Methods. Labelings with anti-DmsA antibody (A), affinity-purified DmsA antibody (B), and anti-DmsB antibody (C) are shown.

may reflect the inherent stability of the enzyme in a lipid bilayer environment or the effects of Triton X-100 on protein conformation. The enzyme in spheroplasts was not accessible to protease. Membrane-bound fumarate reductase was readily proteolysed at pH 7.0 and 30°C, whereas DMSO reductase required a combination of higher temperature, higher pH, and solubilizing agents. The relative stability of the DMSO reductase to proteolysis suggests a compact tertiary structure. The association of bound lipids or carbohydrates is often implicated in the stability of the enzymes; however, we were not able to detect any lipids or carbohydrates stoichiometrically bound to the reductase (data not shown).

The absence of a convenient membrane-bound marker enzyme of the periplasmic space has hindered probing of this aspect of the plasma membrane. Right side out vesicles prepared by the Kaback procedure (21) were found to be unsuitable in the experiments on antibody-mediated agglutination of membrane vesicles. The vesicles undergo lysis and nonspecific agglutination during incubation with antibodies.

TABLE 1. Distribution of DMSO reductase as seen by immunogold labeling[a]

Antibody	No. of gold particles (%)[b]	
	Inner membrane	Cytoplasm
Anti-DmsABC	78 ± 12 (70)	33 ± 9 (30)
Anti-DmsA	76 ± 14 (61)	48 ± 19 (39)
Anti-DmsB	27 ± 6 (59)	19 ± 7 (41)

[a] These studies were carried out in Lowicryl-embedded thin sections from HB101(pDMS159). Gold particles on the electron micrographs obtained for anti-DmsABC (n = 7), anti-DmsA (n = 6), and anti-DmsB (n = 6) antibodies are represented as mean ± standard deviation.

[b] The regions of inner membrane are defined as the 60-nm-wide zone in the vicinity of the inner membrane, as described by Ghosh et al. (14). The region excluding the inner membrane is taken as cytoplasmic zone. Numbers in parenthesis indicate the percent distribution of the gold particles calculated from the mean distribution in the respective zones.

In a fresh right side out vesicle preparation, the accessibilities of fumarate and DMSO reductases to proteases were found to be similar to those of outer membrane-permeabilized cells (Fig. 3). The same vesicles, when subjected to freezing and thawing or incubation with the reductase antibodies for 16 to 18 h, precipitated up to 50% of the membrane-bound reductase activity (data not shown). Addition of Mg^{2+} during the preparation of the vesicles, freeze thawing, strain variations, etc., have been reported to lead to agglutination, altered topology due to flip-flop, and anomalous sedimentation profiles during density gradient centrifugation (13, 21, 31).

Lactoperoxidase-catalyzed iodination of the Dms subunits was observed in everted membranes. The hydropathy profile of DmsC suggests that it is composed of eight transmembranal helical segments and that both surfaces have potential halogenation sites (4). The accessibility of these residues was also verified by another surface-specific iodination reagent, 1,3,4,6-tetrachloro-3α,6α-diphenyl glycoluril (Iodogen) (data not shown). We predict that DmsC anchors the DmsAB subunits to the membrane in much the same manner that FrdCD anchors FrdA and -B (9, 11, 25), and these radioiodination experiments suggest that at least a portion of DmsC is outside the plasma membrane domain.

Negative-stain electron microscopy of everted vesicles confirmed that both DmsA and -B were on the cytoplasmic surface, perhaps existing as a side by side dimer. This model for the structure of DMSO reductase differs from that of fumarate reductase (10, 25) in which the FrdA subunit umbrellas the FrdB subunit, protecting it from iodination and proteolysis (10). Overproduction of DMSO reductase did not induce the biosynthesis of a protein-lipid organelle as was seen with fumarate reductase (12). This may be due to differences in the expression level; fumarate reductase can account for 70 to 90% of the protein in a membrane preparation (10, 39), whereas DMSO reductase never exceeds 30% (40). We also examined the localization of DMSO

reductase in thin sections. The enzyme was clearly associated with the plasma membrane, and examination of the micrographs indicate that both DmsA and B are on the cytoplasmic side.

E. coli expresses several TMAO reductases during anaerobic growth (2, 16, 43), and the relationship of these activities to DMSO reductase has not yet been clarified. The DMSO reductase we are investigating catalyzes TMAO reduction at about three times the rate of DMSO reduction; however, the K_m for TMAO is much higher than the K_m for DMSO (7 versus 0.3 mM). We have constructed a chromosomal deletion mutation lacking all three *dms* genes and have shown that DMSO reductase accounts for about 90% of the TMAO reductase activity observed in anaerobic *E. coli* (Sambasivarao and Weiner, unpublished data). It is thus unlikely that we are monitoring the topology of a different reductase. This argument is further strengthened by the use of antibodies directed against the DmsA and -B subunits which do not cross-react with other proteins.

We found that addition of substrate dramatically improved the association of DmsAB with the membrane and resulted in much better immunogold labeling. Substrate also appears to lock the enzyme in a stable conformation which is very protease resistant. The results indicate that the topology of reductase in the amplified strain is not affected by the overproduction of enzyme. This information is critical to studies on localization of enzymes that demand the use of amplified strains.

The localization of β-lactamase in *E. coli* was shown to be periplasmic both by cell fractionation and electron microscopic techniques. However, when β-lactamase was overproduced, cell fractionation failed to release the enzyme into the supernatant. The enzyme was found to be associated with the membrane fraction, even after sonication. A detailed immunoelectron microscopic characterization of the β-lactamase overproducing strains revealed that the enzyme was found as densely packed periplasmic aggregates (3). In the overproducing strain of DMSO reductase, no such aggregates were seen near the periplasm or in the cytoplasm.

Fumarate reductase, nitrate reductase, and now DMSO reductase are clearly shown to be associated with the cytoplasmic aspect of the plasma membrane. The role of these terminal reductases in the anaerobic electron transport chain is consistent with the predictions of the chemiosmotic hypothesis (6, 10, 19). The bioenergetic role of other periplasmic-soluble reductases needs further attention.

ACKNOWLEDGMENTS

We thank Glen D. Armstrong for helpful discussions, R. D. Bradley for photography, and Douglas P. MacIsaac for the purified DMSO reductase.

This work was supported by grants MT-5838 (to J.H.W.) and MT-8946 (to D.G.S.) from the Medical Research Council of Canada. D. Sambasivarao is postdoctoral fellow of the Alberta Heritage Foundation for Medical Research.

LITERATURE CITED

1. **Ames, G. F.-L., C. Prody, and S. Kustu.** 1984. Simple, rapid, and quantitative release of periplasmic proteins by chloroform. J. Bacteriol. **160**:1181–1183.
2. **Barrett, E. L., and H. S. Kwan.** 1985. Bacterial reduction of trimethylamine oxide. Annu. Rev. Microbiol. **39**:131–149.
3. **Bernadac, A., J.-M. Bolla, C. Lazdunski, M. Inouye, and J.-M. Pages.** 1987. Precise localization of an overproduced periplasmic protein in *Escherichia coli*: use of double immunogold labeling. Biol. Cell. **61**:141–147.
4. **Bilous, P. T., S. T. Cole, W. F. Anderson, and J. H. Weiner.** 1988. Nucleotide sequence of the *dms ABC* operon encoding the anaerobic dimethyl sulfoxide reductase of *Escherichia coli*. Mol. Microbiol. **2**:785–795.
5. **Bilous, P. T., and J. H. Weiner.** 1985. Dimethyl sulfoxide reductase activity by anaerobically grown *Escherichia coli* HB101. J. Bacteriol. **162**:1151–1155.
6. **Bilous, P. T., and J. H. Weiner.** 1985. Protein translocation coupled to dimethyl sulfoxide reduction in anaerobically grown *Escherichia coli* HB101. J. Bacteriol. **163**:369–375.
7. **Bilous, P. T., and J. H. Weiner.** 1988. Molecular cloning and expression of the *Escherichia coli* dimethyl sulfoxide reductase operon. J. Bacteriol. **170**:1511–1518.
8. **Bragg, P. D., and N. R. Hackett.** 1983. Cytochromes of the trimethylamine N-oxide anaerobic respiratory pathway of *Escherichia coli*. Biochim. Biophys. Acta **725**:168–177.
9. **Broome, S., and W. Gilbert.** 1978. Immunological screening method to detect specific translation products. Proc. Natl. Acad. Sci. USA **75**:2746–2749.
10. **Cole, S. T., C. Condon, B. D. Lemire, and J. H. Weiner.** 1985. Molecular biology, biochemistry and bioenergetics of fumarate reductase, a complex membrane-bound iron-sulfur flavoenzyme of *Escherichia coli*. Biochim. Biophys. Acta **811**:381–403.
11. **Condon, C., and J. H. Weiner.** 1988. Fumarate reductase of *Escherichia coli*: an investigation of function and assembly using *in vivo* complementation. Mol. Microbiol. **2**:43–52.
12. **Elmes, M. L., D. G. Scraba, and J. H. Weiner.** 1986. Isolation and characterization of the tubular organelles induced by fumarate reductase overproduction in *Escherichia coli*. J. Gen. Microbiol. **132**:1429–1439.
13. **Futai, M.** 1978. Experimental systems for the study of active transport in bacteria, p. 7–41. *In* B. P. Rosen (ed.), Bacterial transport. Marcel Dekker, Inc., New York.
14. **Ghosh, B. K., K. Owens, R. Pietri, and A. Peterkofsky.** 1989. Localization of the inner surface of the cytoplasmic membrane by immunoelectron microscopy of enzyme I of the phosphoenol pyruvate: sugar phosphotransferase system of *Escherichia coli*. Proc. Natl. Acad. Sci. USA **86**:849–853.
15. **Graham, A., and D. H. Boxer.** 1981. The organization of formate dehydrogenase in the cytoplasmic membrane of *Escherichia coli*. Biochem. J. **195**:627–637.
16. **Haddock, B. A., and C. W. Jones.** 1977. Bacterial respiration. Bacteriol. Rev. **41**:47–99.
17. **Hare, J. F., K. Olden, and E. P. Kennedy.** 1974. Heterogeneity of membrane vesicles from *Escherichia coli* and their subfractionation with antibody to ATPase. Proc. Natl. Acad. Sci. USA **71**:4843–4846.
18. **Hunkapiller, M. W., E. Lujan, F. O. Strander, and L. E. Hood.** 1983. Isolation of microgram quantities of protein from polyacrylamide gels for amino acid sequence analysis. Methods Enzymol. **91**:227–236.
19. **Ingledew, W. J., and R. K. Poole.** 1984. The respiratory chains of *Escherichia coli*. Microbiol. Rev. **48**:222–271.
20. **Jones, R. W., and P. B. Garland.** 1977. Sites and specificity of the reaction of bipyridium compounds with anaerobic respiratory enzymes of *Escherichia coli*: effects of permeability barriers imposed by the cytoplasmic membrane. Biochem. J. **164**: 199–211.
21. **Kaback, H. R.** 1971. Bacterial membranes. Methods Enzymol. **22**:99–120.
22. **Kroger, A., E. Dorrer, and E. Winkler.** 1980. The orientation of the substrate sites of formate dehydrogenase and fumarate reductase in the membrane of *Vibrio succinogenes*. Biochim. Biophys. Acta **589**:118–136.
23. **Kurihara, F. N., and T. Satosh.** 1988. A single enzyme is responsible for both dimethylsulfoxide and trimethylamine N-oxide respirations as the terminal reductase in a photodenitrifier, *Rhodobacter sphaeroides f.s. dentrificans*. Plant Cell Physiol. **29**:377–379.
24. **Laemmli, U. K.** 1970. Cleavage of structural proteins during the assembly of the head of bacteriophage T4. Nature (London) **227**:680–685.
25. **Lemire, B. D., J. J. Robinson, R. D. Bradley, D. G. Scraba, and**

J. H. Weiner. 1983. Structure of fumarate reductase on the cytoplasmic membrane of *Escherichia coli*. J. Bacteriol. **155:** 391–397.
26. **Manoil, C., and J. Beckwith.** 1985. TnphoA: a transposon probe for protein export signals. Proc. Natl. Acad. Sci. USA **82:**8129–8133.
27. **Markwell, M. A. K., S. M. Haas, L. L. Bieber, and N. E. Tolbert.** 1978. A modification of the Lowry procedure to simplify protein determination in membrane and lipoprotein samples. Anal. Biochem. **87:**206–210.
28. **McEwan, A. G., H. G. Wetzstein, S. J. Ferguson, and J. B. Jackson.** 1985. Periplasmic location of the terminal reductase in trimethylamine N-oxide and dimethylsulfoxide respiration in the photosynthetic bacterium *Rhodopseudomonas capsulata*. Biochim. Biophys. Acta **806:**410–417.
29. **Morrison, M.** 1974. The determination of the exposed proteins on membranes by the use of lactoperoxidase. Methods Enzymol. **32:**103–109.
30. **Neu, H. C., and L. A. Heppel.** 1965. The release of enzymes from *Escherichia coli* by osmotic shock and during the formation of spheroplasts. J. Biol. Chem. **240:**3685–3692.
31. **Osborn, M. J., and R. Munson.** 1974. Separation of the inner (cytoplasmic) and outer membranes of gram-negative bacteria. Methods Enzymol. **31:**642–653.
32. **Pascal, M.-C., J.-F. Burini, and M. Chippaux.** 1984. Regulation of the trimethylamine N-oxide (TMAO) reductase in *Escherichia coli*: analysis of tor::Mud1 operon fusion. Mol. Gen. Genet. **195:**351–355.
33. **Renart, J., J. Reiser, and G. R. Stark.** 1979. Transfer of proteins from gels to diazobenzyloxymethyl-paper and detection with antisera: a method for studying antibody specificity and antigen structure. Proc. Natl. Acad. Sci. USA **76:**3116–3120.
34. **Rosen, B. P., and T. Tsuchiya.** 1979. Preparation of everted membrane vesicles from *Escherichia coli* for the measurement of calcium transport. Methods Enzymol. **56:**233–241.
35. **Roth, J.** 1986. Post-embedding cytochemistry with gold-labelled reagents: a review. J. Microsc. (Paris) **143:**125–137.
36. **Shimokawa, O., and M. Ishimoto.** 1979. Purification and some properties of inducible tertiary amine N-oxide reductase from *Escherichia coli*. J. Biochem. **86:**1709–1717.
37. **Smith, D. E., and P. A. Fisher.** 1984. Identification, developmental regulation, and response to heat shock for two antigenically related forms of a major nuclear envelope protein in Drosophila embryos: application of an improved method for affinity purification of antibodies using polypeptides immobilized on nitrocellulose blots. J. Cell Biol. **99:**20–28.
38. **von Heijne, G., W. Wickner, and R. E. Dalbey.** 1988. The cytoplasmic domain of *Escherichia coli* leader peptidase is a "translocation poison" sequence. Proc. Natl. Acad. Sci. USA **85:**3363–3366.
39. **Weiner, J. H., B. D. Lemire, M. L. Elmes, R. D. Bradley, and D. G. Scraba.** 1984. Overproduction of fumarate reductase in *Escherichia coli* induces a novel intracellular lipid protein organelle. J. Bacteriol. **158:**590–596.
40. **Weiner, J. H., D. P. MacIsaac, R. E. Bishop, and P. T. Bilous.** 1988. Purification and properties of *Escherichia coli* dimethylsulfoxide, an iron-sulfur molybdo enzyme with broad substrate specificity. J. Bacteriol. **170:**1505–1510.
41. **Wolfe, P. B., W. Wickner, and J. M. Goodman.** 1983. Sequence of the leader peptidase gene of *Escherichia coli* and the orientation of leader peptidase in the bacterial envelope. J. Biol. Chem. **258:**12073–12080.
42. **Yamamoto, I., N. Okubo, and M. Ishimoto.** 1986. Further characterization of trimethylamine N-oxide reductase from *Escherichia coli*, a molybdoprotein. J. Biochem. **99:**1773–1779.
43. **Yamamoto, I., M. Hinakura, S. Seki, Y. Seki, and H. Kondo.** 1989. Reduction of N-oxide and S-oxide compounds by *Escherichia coli*. J. Gen. Appl. Microbiol. **35:**253–259.
44. **Yamato, I., Y. Anraku, and K. Hirosawa.** 1975. Cytoplasmic membrane vesicles of *Escherichia coli*: a simple method for preparing the cytoplasmic and outer membranes. J. Biochem. **77:**705–718.